Quantification of Recruitment Properties of Multiple Contact Cuff Electrodes

Warren M. Grill Jr., *Member, IEEE,* and J. Thomas Mortimer

***Abstract*—Nerve-based stimulating electrodes provide the technology for advancing the function of motor system neural prostheses. The goal of this work was to measure and quantify the recruitment properties of a 12 contact spiral nerve cuff electrode. The cuff was implanted on the cat sciatic nerve trunk, which consists of at least four distinct motor fascicles, and the torque generated at the ankle joint by selective stimulation of the nerve was recorded in nine acute experiments. Comparisons of torques generated with the cuff to torques generated by selective stimulation of individual nerve branches indicated that the cuff allowed selective activation of individual nerve fascicles. Selectivity was dependent on the relative location of the electrode contacts and the nerve fascicles, as well as the size and relative spacing of neighboring fascicles. Selective stimulation of individual nerve fascicles allowed independent and graded control of dorsiflexion and plantarflexion torques in all nine experiments. Field steering currents improved selectivity as reflected by significant increases in the maximum torques that could be generated before spillover to other fascicles, significant increases in the difference between the current amplitude at spillover and the current amplitude at threshold, and significant increases in the slope of the current distance relationship.**

***Index Terms*— Neural stimulation, neural prostheses, recruitment, electrodes, cat, sciatic nerve.**

I. Introduction

ELECTRICAL stimulation of the nervous system is a method to restore function to individuals with neurological impairments [18], [24]. For example, activation of paralyzed muscles by electrical stimulation of intact lower motor neurons allows restoration of movement to persons with spinal cord injury, head injury, or stroke [32]. Clinical applications of this technology, known as motor prostheses, include electrical activation of the peroneal nerve to correct footdrop [42], electrical activation of the sacral ventral roots to empty the bladder [3], [31], electrical activation of the phrenic nerve for respiration [8], [34], [35], and activation of the upper and lower extremities for functional movement [32]. In each of these applications, at least one electrode is used to activate each muscle. Although control of larger numbers of muscles should increase prosthesis function and allow application of devices to a larger patient population, with current technology this requires implantation and maintenance of a large number of electrodes.

To reduce the number of implanted electrodes in advanced motor prostheses, electrodes are required that can stimulate independently several muscles [27]. Selective stimulation of individual components of multifascicular peripheral nerves would allow control of larger number of muscles with less implanted hardware. Electrodes currently under development for selective activation of peripheral nerves include intraneural wire and silicon electrodes [21], [30], [39], [43], epineural electrodes [35], [37], and multiple contact nerve cuff electrodes [27], [41]. The feasibility of selective activation of peripheral nerve fascicles was demonstrated by McNeal and Bowman [25] who found that with proper fit and positioning a single circumneural sleeve with multiple electrode contacts could control selectively the activation of two antagonist muscle groups innervated by a common nerve trunk. Sweeney *et al.* demonstrated selective activation of an individual nerve fascicle with carefully chosen electrode positions, and pioneered the use of sub-threshold field steering currents to improve selectivity [33]. More recently, we developed a 12-contact spiral nerve cuff electrode that allowed selective activation of individual peripheral nerve fascicles [41]. Thus, a multiple contact cuff electrode may provide the technology to advance the function of motor prostheses with less implanted hardware [27].

The objective of this study was to quantify the input-output properties of the 12-contact spiral cuff electrode. As in our previous study, electrodes were implanted without prior reference to nerve fascicle location, and no effort was made to tune the stimulus parameters to achieve selective activation of a particular nerve component. However, rather than recording the force developed in a select subset of muscles as done in our previous work, the net torque generated at the ankle joint was the recorded output variable. Records of joint torque were combined with maps of the sciatic nerve topography to determine which components of the nerve were activated by a particular stimulus paradigm. This information, termed "neuronal selectivity," was independent of the system under study, and was only a function of the nerve and electrode geometry. The range of torques that could be generated at the ankle joint was also quantified. This information, termed "functional selectivity," was system specific and indicated the performance of the electrode in the particular application of controlling ankle joint torque. This study further documents the selectivity of multiple contact cuff electrodes, and provides input-output relations necessary for development of control

Manuscript received April 28, 1995; revised March 4, 1996. This work was supported in part by a grant from the Paralyzed Veterans of America Spinal Cord Research Foundation and by NIH-NINDS Neural Prosthesis Program Contract N01-NS-3-2300.

The authors are with the Applied Neural Control Laboratory, Department of Biomedical Engineering, Case Western Reserve University, Cleveland, OH 44106 USA (Grill e-mail: wmg@po.cwru.edu; (Mortimer e-mail: jtm3@po.cwru.edu).

Publisher Item Identifier S 1063-6528(96)04247-4.

methods using these electrodes. Some results of these studies have been published in abstract form [12], [14].

II. Methods

A. Experimental Procedure

Nine acute experiments were conducted on adult cats. All animal care and experimental procedures were according to NIH guidelines and were approved by the Institutional Animal Care and Use Committee of Case Western Reserve University. Animals were initially anesthetized with ketamine hydrochloride (35 mg/kg, I.M.), and atropine sulfate (0.05 mg/kg, I.M.) was administered to reduce airway secretions. A catheter was inserted in the cephalic vein, and a surgical level of anesthesia was maintained throughout the experiment with sodium pentobarbital (5–10 mg bolus injections, I.V.). Animals were intubated and body temperature was maintained with a heating pad. Warm Ringer's solution (10 cc/kg/h) was administered during the experiment. The sciatic nerve was exposed through a dorsal approach and mobilized over several centimeters proximal to the popliteal fossa. The nerve circumference was measured with a piece of 6-0 polypropylene suture, and the equivalent nerve diameter was calculated assuming a circular nerve cross-section. A silicone rubber spiral cuff electrode containing 12 individually addressable platinum contacts [41] was implanted on the right $(n = 8)$ or left $(n = 1)$ sciatic nerve 2–3 cm proximal to the bifurcation into tibial and common peroneal components. The size of the cuff was chosen in each case to place the four tripoles at equal circumferential intervals around to nerve and to provide a snug fit between the cuff and the nerve (range of cuff diameter to nerve diameter ratio was 0.72–0.8). No effort was made to orient the cuff around the nerve, and the location of the four individual tripoles varied from experiment to experiment.

The animal was mounted in the measurement apparatus, as shown in Fig. 1(a), with the ankle, knee, and hip joint angles set to $90 \pm 5°$, $100 \pm 10°$, and $110 \pm 10°$ degrees, respectively [10]. A 3-dimensional (3-D) strain gauge transducer (JR3 Inc., Woodland, CA) was used to measure plantarflexion/dorsiflexion torques, external rotation/internal rotation (toe-out/toe-in) torques, and inversion/eversion torques [Fig. 1(b)]. Details of torque recording methods can be found in [17].

B. Stimulation and Recording

Isometric twitch contractions were generated in the ankle musculature by selective electrical stimulation of the sciatic nerve via the implanted cuff electrode. Tripolar electrode configurations were used and sub-threshold field steering current from an anode 180° around the nerve trunk from the active cathode (transverse steering) was used to modify the region of excitation [Fig. 1(c)]. Tripolar configurations with sub-threshold field steering current from a contact 90° around the nerve trunk from the active cathode (adjacent steering) were also investigated in three experiments [Fig. 1(d)]. All stimuli and steering currents were 10 μs monophasic, rectangular, regulated current pulses delivered at 0.5 Hz from a stimulator designed and built in our laboratory. Current amplitude was set manually with calibrated potentiometers, and pulse duration was controlled by computer. The amplitude

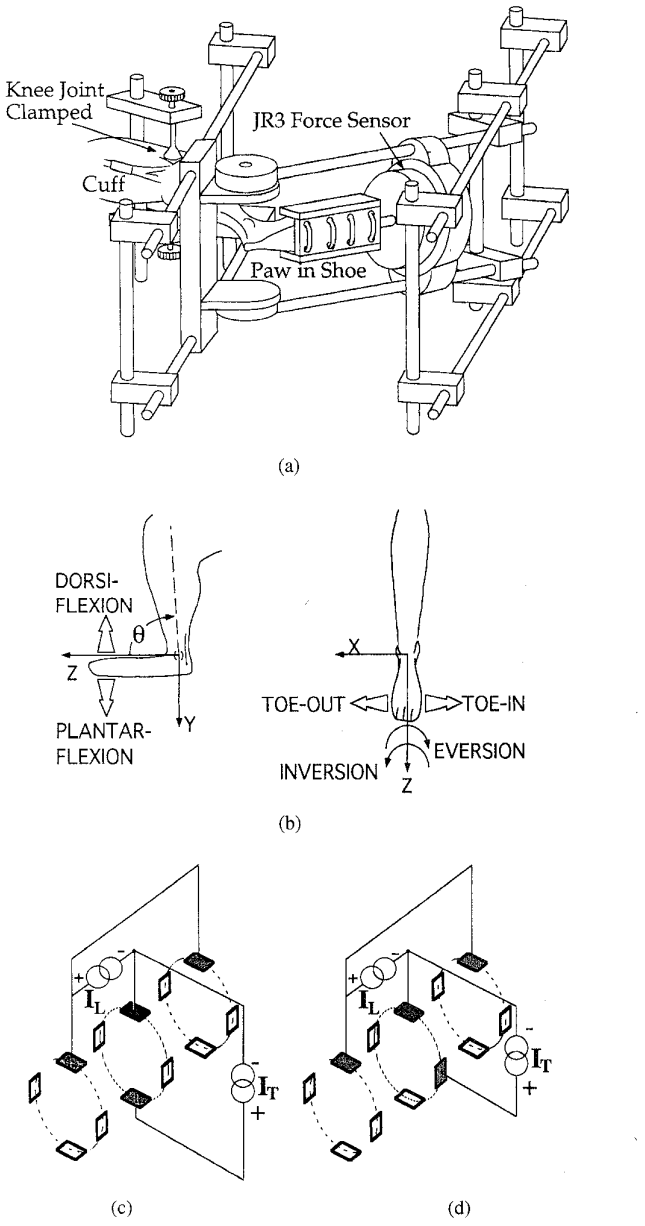

Fig. 1. (a) Experimental apparatus to measure the 3-D isometric torque generated at the cat ankle joint by electrical stimulation of the sciatic nerve. The paw was fixed in an aluminum shoe with plastic tie wraps and the knee was immobilized with a pair of clamps. The apparatus allowed the ankle joint angle to be varied in the sagittal plane to measure position-dependent recruitment properties. (b) Diagram of the cat shank and ankle joint showing measurement system coordinates, definitions of torque components, and definition of the ankle joint angle (θ). (c) Longitudinal tripolar electrode configuration with transverse field steering current. The longitudinal stimulus current, I_L, was applied between the cathode (*black*) and two anodes (*gray*). Transverse field steering current, I_T, with an amplitude of 0, 45%, or 90% of the transverse excitation threshold was applied between the cathode and a third anode (*gray*) 180° around from the active cathode. (d) Longitudinal tripolar electrode configuration with adjacent field steering current. The longitudinal stimulus current, I_L, was applied between the cathode (*black*) and two anodes (*gray*). Adjacent field steering current, I_A, with an amplitude of 0, 45%, or 90% of the adjacent excitation threshold was applied between the cathode a third anode (*in gray*) 90° around from the cathode.

of the steering current was set to either 0 ("no steering"), 45% ("45% steering"), or 90% ("90% steering") of either the transverse threshold (1584 ± 570 μA, range $= 480 - 2960$ μA, $n = 36$ in nine experiments) or the adjacent threshold (1743 ± 503 μA, range $= 840 - 2200$ μA, $n = 24$ in three experiments), depending on which configuration was under test. Each of the four tripoles in the cuff (labeled 0°, 90°, 180°, 270°) was tested without and without steering current in every experiment. The torque responses generated by stimulation of the individual branches of the sciatic nerve (tibial, common peroneal, medial gastrocnemius, and lateral gastrocnemius/soleus) with a bipolar hook electrode were also recorded in three experiments. The torque signals were low-pass filtered at 100 Hz and sampled at 200 Hz with a 12-b A/D converter. Five twitch responses were collected at each stimulus amplitude and were averaged. Stimulus control and torque response sampling were accomplished using a multiple function input output board (NB-MIO-16H, National Instruments, Austin, TX) and software written in LABView running on a Macintosh Quadra 950.

C. Morphological Mapping

At the conclusion of each experiment the location of each tripole was marked on the nerve trunk by inserting sutures into the epineurium. The distal branches of the sciatic nerve were identified by dissection and stimulation, the branches were labeled, and the cuff, nerve, and distal branches were excised. The cuff was removed and the nerve was immersion fixed in a refrigerated solution of 4% formaldehyde and 1.5% methanol in sodium phosphate buffer. After fixation, the nerve was sectioned under a surgical microscope and the fascicles corresponding to each of the branches were identified. The dissection was recorded on videotape for later review. Nerve sections, 5 mm long, were cut at the distal end of the cuff, at the center of the cuff, and at the proximal end of the cuff. These sections were post-fixed in osmium tetroxide, dehydrated in acetone series, and embedded in Spurr's low viscosity resin. Semi-thin (1 μm) transverse sections were cut, stained with methylene blue borax, coverslipped, and examined using a light microscope.

Microscopic images of transverse nerve sections were digitized and traced using a computer-based image processing system. Information about electrode position and fascicle identification from the dissection was used to construct morphological maps using the digitized images. The spacing between the tripoles was determined *a priori* by the cuff size, and this information was used to limit errors due to the suture placement. To examine the errors due to tissue shrinkage, nerve diameters were measured from nerve sections and compared to diameters obtained *in situ*. There were no significant differences between these measurements (mean absolute difference $= 0.06$ mm, $p = 0.375$, paired sign test, $n = 9$), and thus tissue shrinkage did not introduce an error in construction of the maps. Using the morphological reconstructions, electrode-to-fiber distances were measured from the center of each central cathode to the closest point on each of the fascicles and from the closest edge of each central cathode to the closest point on each of the fascicles.

D. Quantification of Recruitment Properties

Three types of information were used to determine which component(s) of the sciatic nerve were activated with a particular electrode configuration and set of stimulus parameters (Fig. 2): recruitment curves of plantarflexion/dorsiflexion (PF/DF) torque as a function of the stimulus current amplitude; the magnitude and direction of the 2-D joint torque vector in the PF/DF versus external rotation/internal rotation (ER/IR) plane; and the shape of the torque twitch waveforms. These data were also related to the locations of the electrode contacts and nerve fascicles using the morphological reconstructions. The peak of the torque twitch was used as a measure of muscle activation because previous analysis indicated that there was a strong linear correlation between the peak of the twitch and the area under the twitch-time curve, even for muscles containing a mixture of motor unit contraction speeds [17].

Recruitment curves of plantarflexion/dorsiflexion torque as a function of stimulus current amplitude were parameterized to quantify electrode performance. Threshold was defined as the lowest current required to elicit either plantarflexion or dorsiflexion torque greater than 2 N-cm. Current amplitude at spillover was defined as the lowest current required to cause activation of a second nerve fascicle. For spillover to an antagonist, this point was identified by a reversal in the sign of the slope of the recruitment curve. For spillover to an agonist, this point was identified by an inflection in the recruitment curve where the slope increased to a value greater than 0.3 N-cm/μA, and confirmed by a change in the direction of the joint torque vector (see below). The difference between the threshold current and the current at spillover was defined as the dynamic range. Additionally, the width(s) of the plateau region(s) of each recruitment curve, defined as regions of saturation where the recruitment gain was $\leq$0.05 N-cm/μA, were determined. Maximum dorsiflexion or plantarflexion torque before spillover and recruitment gain were also determined for each recruitment curve. To calculate the normalized recruitment gain (NRG), recruitment curves were first truncated at the point of antagonist spillover such that the slope did not reverse sign over the curve. The torque values of each recruitment curve were then normalized so the maximum torque was equal to 1, and current amplitudes were normalized so threshold was equal to 1 Normalization in this manner eliminated any coupling between threshold or maximum torque and recruitment gain. NRG was defined as the instantaneous slope of the normalized recruitment curve [11], and the mean, standard deviation, and range of NRG were determined over each recruitment curve.

The positional stability of recruitment properties was determined by comparing recruitment curves of PF/DF torque measured at different ankle joint positions. To isolate the position dependent recruitment properties of the cuff electrode, each recruitment curve was first normalized so that the maximum torque at each ankle joint angle was equal to 1. Normalization in this manner [5] eliminated the scaling due to length-tension properties of skeletal muscle [28] and joint-angle-dependent moment arms [44]. The normalized torque at $\pm 20°$ was plotted as a function of the normalized torque at 90°

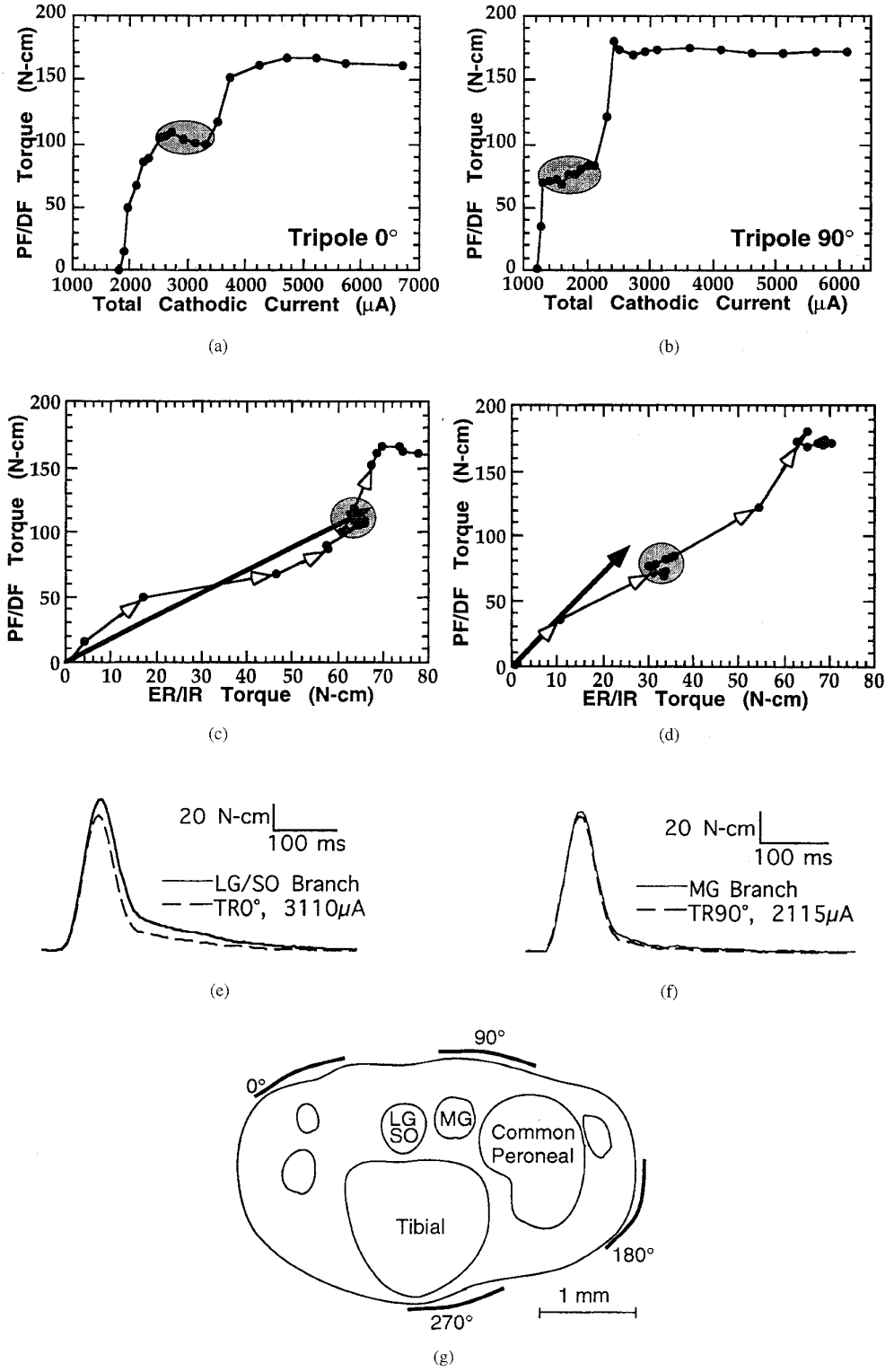

Fig. 2. Evoked joint torque was used to determine what component(s) of the sciatic nerve were activated with an electrode configuration and set of stimulus parameters. (a) and (b) Recruitment curves of plantarflexion/dorsiflexion (PF/DF) torque as a function of the total cathodic current (i.e., stimulus + steering) for two neighboring tripoles (0°, 90% steering = 1710 μA, and 90°, 90% steering = 1116 μA). (c) and (d) 2-D vector plots of the recruitment data from the same two tripoles in the PF/DF versus external rotation/internal rotation (ER/IR) plane. Each point indicates the tip of the joint torque vector and the line with the open arrowheads indicates the trajectory through torque space with the stimulus current amplitude as the path variable. The clusters of points (shaded regions) correspond to the plateau regions of the recruitment curves. The bold arrows are the torque vectors generated by supra-maximal activation with a hook electrode distal to the cuff of either the lateral gastrocnemius/soleus (LG/SO) nerve branch (c) or the medial gastrocnemius (MG) nerve branch (d). (e) and (f) Torque twitch waveforms evoked with the cuff electrode or by supramaximal stimulation of individual nerve branches with a hook electrode. (g) Morphological reconstruction of the cross section of the sciatic nerve at the center of the cuff electrode indicating the location of each fascicle and each electrode contact.

with current as the independent variable. Position dependent recruitment was quantified by determining the deviations of the measured points from the unity slope line, expressed as a percentage of the maximum torque [5].

Recruitment data were also plotted as vectors in the plantarflexion/ dorsiflexion versus external rotation/internal rotation plane to examine the 2-D torque vector generated at the ankle joint. Points of spillover to agonist or antagonist muscles could be identified by a change in the direction of the 2-D joint torque vector. The range of vector directions was calculated as the difference between the maximum and minimum vector directions (in degrees) between threshold and spillover. The range of joint torque vector directions was small before spillover ($14.5° \pm 22.3°$, $n = 36, 9$), but after spillover the range of vector directions increased significantly ($66.3° \pm 82°$, $p = 0.0009$). Although ankle inversion/eversion torques were also recorded, the magnitude of these torques was always less than 5 μ-cm and they were not included in these analyses [22].

Comparisons of recruitment with and without steering current were analyzed with respect to the total cathodic current. This was the total current (stimulating + steering) that entered the cathode of the tripole. Statistical comparisons for experimental groups of less than 15 samples were made using the nonparametric sign test [26]. Statistical tests on larger samples were made using a two tailed, paired t-test [26]. All parameters are presented in the format 'mean $\pm$ standard deviation' with the sample size indicated as '# of recruitment curves, # of experiments'.

III. Results

The ankle joint torque evoked by selective stimulation of the sciatic nerve was a nonlinear function of the stimulus current amplitude. Recruitment curves of plantarflexion/dorsiflexion (PF/DF) torque had a sigmoidal shape during activation of a single fascicle, and the magnitude of the torque was a monotonically increasing function of stimulus amplitude (e.g., Figs. 2 and 3). Plateau regions of joint torque recruitment curves indicated selective and complete activation of nerve fascicles. When activation spread to the innervation of an agonist, the recruitment curve had a second region where the magnitude of the torque was again a monotonically increasing function of stimulus amplitude [e.g., Fig. 3(a) and (b)]. This pattern was observed in 32/94 (34%) curves. When spread of activation to the innervation of an antagonist occurred, the magnitude of the net torque decreased and in some cases changed sign [e.g., Fig. 3(f)]. This pattern was observed in 60/94 (64%) curves. The remaining two curves (2%) exhibited no spillover. Some recruitment curves (36/94, 38%) had secondary regions of spillover where a third component of the nerve was recruited.

A. Neuronal Selectivity

1) Fascicle Selective Activation: Separate tripoles allowed selective activation of individual nerve fascicles as indicated by plateaus in the PF/DF torque recruitment curve and clusters of joint torque vectors in the PF/DF versus external rotation/internal rotation (ER/IR) plane. An example of the recruitment properties of two neighboring tripoles is shown in Fig. 2. The PF torque generated by tripole 0° with 90% transverse steering current [Fig. 2(a)] increased to a plateau value (*shaded region*) followed by a second increase in torque at total current amplitudes greater than 3300 μA. Similarly, the PF torque generated by tripole 90° with 90% steering [Fig. 2(b)] increased to a plateau value (*shaded region*) followed by a second increase in torque at total current amplitudes greater than 2200 μA. Both of these patterns indicated recruitment of one fascicle to saturation (plateau region), followed by spillover to the innervation of an agonist muscle.

There was a consistent correspondence between plateaus in the PF/DF recruitment curve and clusters of points in the joint torque plane. The 2-D joint torque vectors generated by the same two tripoles described above are shown in Fig. 2(c) and (d). Each point indicates the tip of the joint torque vector generated at a particular stimulus current amplitude, and the line with the open arrowheads indicates the trajectory through torque space as the stimulus current amplitude was increased (i.e., the stimulus current amplitude was the path variable). The clusters of vectors (shaded regions) in the plane correspond to the plateau regions of the recruitment curves of Fig. 2(a) and (b) (see also Fig. 3 and [17]).

Comparisons between the torques generated using stimuli applied with the cuff and the torques generated by selective stimulation of individual nerve branches with a hook electrode confirmed that plateau regions and torque vector clusters indicated selective activation of individual nerve fascicles. The bold arrows in Fig. 2(c) and (d) are the ankle joint torque vectors generated by supra-maximal stimulation of either the lateral gastrocnemius (LG)/soleus (SO) nerve branch [Fig. 2(c)] or the medial gastrocnemius (MG) nerve branch [Fig. 2(d)] distal to the cuff with a hook electrode. The clusters of vectors generated with the cuff electrode (i.e., points from the plateau region) corresponded to the vectors generated by selective activation of the muscle branches. Thus, the cluster of vectors generated by tripole 0° indicated that the first recruited fascicle (LG/SO) was fully activated before the stimulation spread to another fascicle. This corresponded to the plateau in the recruitment curve between 2600 μA and 3300 μA [Fig. 2(a)]. The cluster of vectors generated by tripole 90° indicated that the first recruited fascicle was the MG. Again, this corresponded to the plateau in the recruitment curve between 1100 μA and 2200 μA [Fig. 2(b)]. In three experiments where cuff and branch stimulation were compared, the differences between the maximum PF/DF torque generated by branch stimulation and the maximum PF/DF torque generated with the cuff were small (mean difference = 4.4 N-cm, $n = 9$, $p = 0.18$). Similarly, there were small differences in the lengths and directions of the torque vectors generated by branch and cuff stimulation (mean length difference = 7.0 N-cm, $p = 0.51$, mean directional difference = 1.8°, $p = 0.18$). Selective activation of individual fascicles was further supported by the shape of torque twitch waveforms. Examples of PF torque twitches evoked with the cuff electrode and those generated by stimulation of individual branches with the hook electrode are shown in Fig. 2(e) and (f). The shape and amplitudes of the

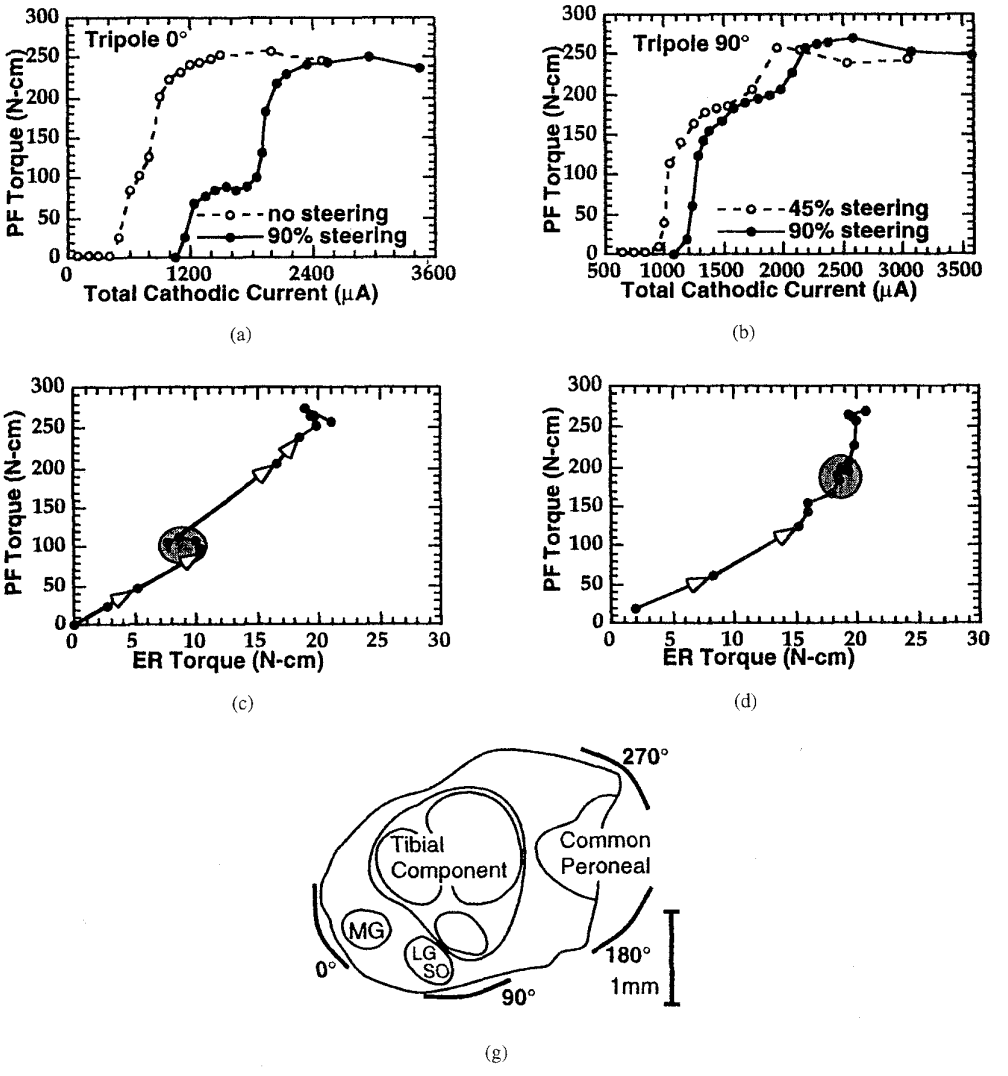

Fig. 3. Selectivity between different fascicles within the nerve trunk was a function of the relative locations of the electrode contacts and the nerve fascicles. (a) and (b) Recruitment curves for two neighboring tripoles of plantarflexion/dorsiflexion (PF/DF) torque as a function of the total cathodic current (i.e., stimulus + steering). 90% steering = 945 μA for tripole 0° and 1080 μA for tripole 90°. (c) and (d) 2-D vector plots of the recruitment data from the same two tripoles, using 90% steering, in the PF/DF versus external rotation/internal rotation (ER/IR) plane. The clusters of points (shaded regions) correspond to the plateau regions of the recruitment curves. (e and f) Recruitment curves of PF/DF torque as a function of the total cathodic current (i.e., stimulus + steering) for two opposite tripoles in another cuff electrode. 90% steering = 954 μA for tripole 0° and 930 μA for tripole 180°. (g and h) Morphological reconstruction of the cross section of the sciatic nerve at the center of the cuff electrode indicating the location of each fascicle and each electrode contact for the experiments shown in A–D (g) and E–F (h) (abbreviations as in Fig. 2, PL = innervation of plantaris).

torque twitches generated with the cuff correspond very well to the twitches generated by stimulation of individual branches with a hook electrode (see also [17]).

Joint torque records were combined with neuronal topography to determine the component(s) on the nerve that were activated in each experiment. A summary of the activation of each fascicle, as well as simultaneous activation of the agonists MG + LG/SO, generated in each of the nine experiments is provided in Table I. The values in the table are the width, in μA, of the plateau region of the recruitment curves of PF/DF torque. Non-zero entries indicate that a fascicle could be activated to produce a plateau torque which, as seen above, corresponded to a cluster of points in the torque vector plane, and selective activation of a particular fascicle. The magnitude of the value indicates the degree of separation between activation of the first recruited and second recruited fascicles. Zero entries indicate that the fascicle could not be activated to a plateau value before spillover occurred; however, they do not necessarily imply that a fascicle could not be activated selectively. For example, compare the two recruitment curves in Fig. 3(a). The plateau in the 90% steering curve clearly indicates selective activation of MG, but although no plateau is present without steering, MG was activated selectively at low current amplitudes ($\leq$700 μA). Therefore, the plateau width is a conservative measure of the degree of isolation for each fascicle.

2) Current Distance Relationship: Selectivity between different fascicles within the nerve trunk was a function of the relative locations of the electrode contacts and the nerve fascicles. When neighboring fascicles were positioned under different

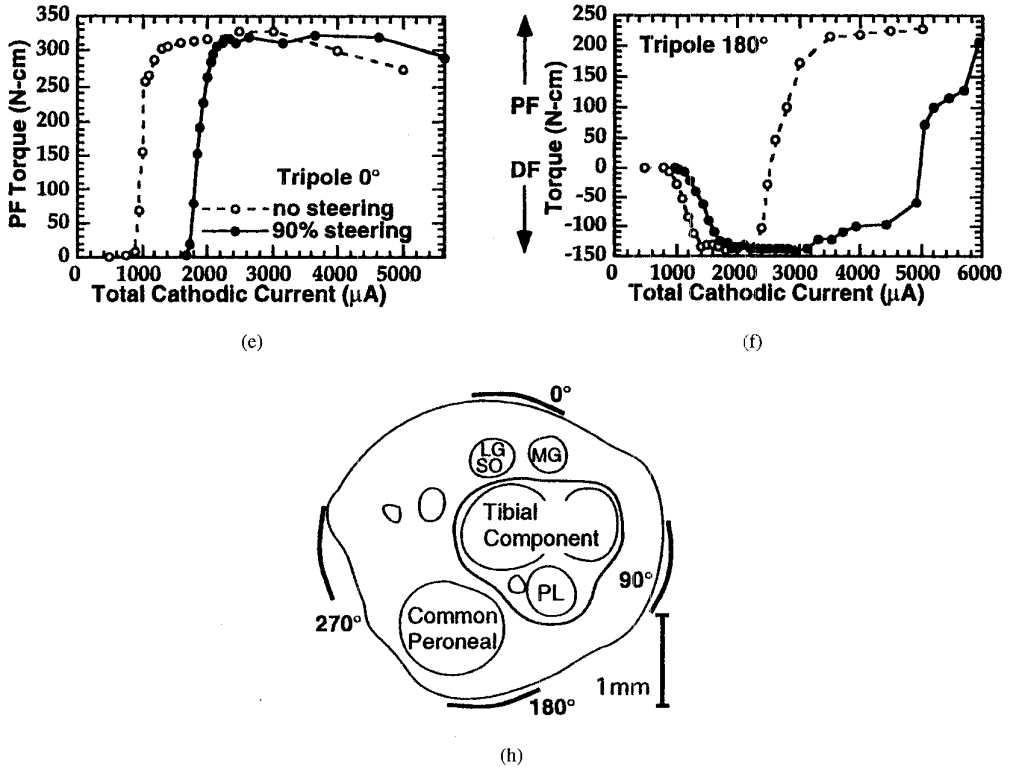

Fig. 3. *(Continued.)* (e and f) Recruitment curves of PF/DF torque as a function of the total cathodic current (i.e., stimulus + steering) for two opposite tripoles in another cuff electrode. 90% steering = 954 μA for tripole 0° and 930 μA for tripole 180°. (g and h) Morphological reconstruction of the cross section of the sciatic nerve at the center of the cuff electrode indicating the location of each fascicle and each electrode contact for the experiments shown in A–D (g) and E–F (h) (abbreviations as in Fig. 2, PL = linnervation of plantaris).

tripoles [Fig. 3(g)], it was possible to activate selectively each of the fascicles using one or the other tripole [Fig. 3(a) and (b)]. In this example, tripole 0° with 90% transverse steering selectively recruited the MG fascicle as shown by the plateau in the recruitment curve and cluster of points in the joint torque plane [Fig. 3(c)]. At higher stimulus amplitudes activation spread to LG/SO. Conversely, tripole 90° with 90% steering initially recruited the LG/SO fascicle as indicated by the plateau region in the recruitment curve [Fig. 3(b)] and the cluster of joint torque vectors [Fig. 3(d)], and at higher currents stimulation spread to MG. This complementary recruitment pattern was consistent with the neighboring locations of the MG and LG/SO fascicles [Fig. 3(g)]. When two fascicles were positioned directly under the same tripole [Fig. 3(h)], both fascicles were activated together. Although transverse field steering current had little effect on selectivity in these situations [Fig. 3(e)], adjacent field steering current improved selectivity between neighboring fascicles (see below).

The relationship between the threshold current to activate a fascicle and the location of the fascicle was quantified using the recruitment data and measurements from the morphological reconstructions of the distance between the electrode contact and each fascicle. The threshold current as a function of the distance between the center of the cathodic electrode contact and the recruited fascicle is shown in Fig. 4(a) (n = 76 measurements in nine experiments). As expected, larger stimulus amplitudes were required to excite nerve fascicles that lay further from the electrode contacts. Both linear ($I_{\rm th}(x) = a + bx$, x is electrode to fascicle distance and a and b are constants) and nonlinear ($I_{\rm th}(x) = a + bx^2$) regression lines were fit to the current-distance data. Correlation analysis indicated that approximately 50% of the variation of the threshold current could be attributed to the electrode to fiber distance (r^2 = 0.47 without steering and r^2 = 0.50 with steering). A similar relationship was found for the nonlinear regression (r^2 = 0.43 without steering and r^2 = 0.49 with steering). Transverse steering current generated a steeper relationship between the threshold current and the electrode to fiber distance. The slopes of the linear regression lines were 801 μA/mm for no steering versus 1328 μA/mm for 90% steering (p = 0.0001, to reject that either slope was equal to zero, p = 0.0068 to reject that slopes were equal).

3) Threshold Difference Between Neighboring Fascicles: The pattern of spillover was dependent on the relative positions of the different fascicles. An example of this is seen clearly in Fig. 3(f). In this case, the common peroneal (CP) fascicle, which was closest to the active tripole, was recruited at the lowest current levels, generating dorsiflexion torque at the ankle joint. At higher currents (above 3000 μA for the "90% steering" curve in Fig. 3(f)], the stimulus spread to activate the next closest fascicle, plantaris (PL), which produced a reduction in the magnitude of the net torque due to its

TABLE I
SUMMARY OF FASCICLE SELECTIVITY

EXP #	MG	LG/SO	MG+ LG/SO	CP	TIB
1	300	300	600	100	0
2	100	0	3000	600	1000
3	850	0	2300	1200	0
4	800	800	1300	200	0
5	100	0	400	100	1500
6	0	500	0	600	800
7	0	0	2600	2000	1500
8	400	900	0	0	2400
9	200	0	700	800	400
mean	306	278	1211	722	844
s.d.	323	370	700	628	840
cases	7/9 (78%)	4/9 (56%)	7/9 (78%)	8/9 (89%)	6/9 (67%)

Each entry in the table is the width, in μA, of the plateau region of the recruitment curves of plantarflexion/dorsiflexion torque as a function of the stimulus current amplitude. Nonzero entries indicate that a fascicle could be activated to produce a plateau torque (slope $\leq$0.05-cm/μA, and the magnitude of the value indicates the degree of separation between activation of the first and second recruited fascicles. Zero entries indicate that the fascicle could not be activated to a plateau value before spillover occurred. (MG =medial gastrocnemius, LG/SO=lateral gastrocnemius/soleus, MG+LG/SO= activation of both fascicles, CP=common peroneal, TIB=tibial.

plantarflexion torque generation (i.e., co-contraction) [1]. As the stimulus amplitude was further increased [above 4500 μA in Fig. 3(f)] the stimulus spread further to cause activation of the MG and LG/SO fascicles and generate a net PF torque. Thus, the spillover patterns could be correlated with the relative locations of the electrode contacts and the nerve fascicles.

The difference between the threshold currents for pairs of fascicles activated by the same tripole is plotted in Fig. 4(b) as a function of the difference in the distances from each fascicle to the center of the electrode contact ($n = 30$ pairs of measurements where the spillover fascicle could be identified). Each point represents two fascicles that were activated by the same tripole at either the same ($n = 2$ cases where the threshold difference was zero) or different current amplitudes. Linear regression lines were calculated for the data without transverse steering current and the data with transverse steering current. The positive slopes of the regression lines ($p = 0.0013$ for no steering, $p = 0.0001$ for 90% steering, reject that slope was equal to zero) indicated that the larger the spatial separation between the fascicles, the larger the difference in their threshold currents. Use of transverse field steering current created larger differences in the thresholds between neighboring fascicles. This was reflected as a steeper slope of the regression line fit to the points with steering current (655 μA/mm without steering versus 1541 μA/mm with steering, $p = 0.0005$, reject that slopes were equal). However, correlation analysis indicated that only 30 to 40% of the variation in the threshold difference could be accounted for by the difference in the distance from each fascicle to the electrode contact ($r^2 = 0.30$ without steering and $r^2 = 0.42$ with steering).

4) Effects Of Transverse Steering Current on Selectivity: Transverse steering current equal to either 45% or 90% of the transverse excitation threshold altered the torques generated at the ankle joint, reflecting the change in the pattern of

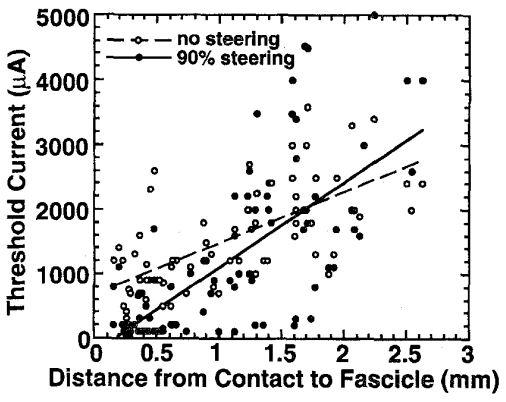

(a)

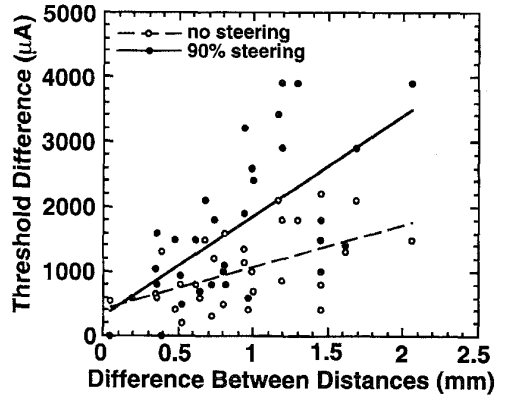

(b)

Fig. 4. Stimulation threshold increased as the distance between the active tripole and the stimulated fascicle increased. (a) Threshold current as a function of the distance between the center of each cathodic electrode contact and the closest point on the active fascicle ($n = 76$ measurements from nine experiments). Linear regression lines are shown for data with ($r^2 = 0.50$) and without ($r^2 = 0.47$) 90% transverse steering current. Transverse field steering current increased the slope of the current distance relationship. (b) Threshold difference between pairs of fascicles plotted as a function of the differences in their respective distances from the center of the electrode contact ($n = 30$ pairs of measurements where spillover could be identified). Linear regression lines are shown for the data with ($r^2 = 0.42$) and without steering current. ($r^2 = 0.30$). Transverse field steering current increased the threshold difference between fascicles.

excitation within the nerve trunk [Fig. 3(a), (b), and (f)]. Two measures were used to quantify the effects of steering current on torque recruitment (see Methods): the dynamic range between the threshold current amplitude and the current amplitude at spillover, and the maximum torque generated before spillover. Transverse steering current increased the dynamic range between threshold and spillover indicating that it limited the spatial extent of stimulation by a particular tripole. Transverse field steering current also increased the maximum torque generated before spillover indicating that more fibers were activated in a localized region of the nerve trunk. These effects were consistent across experiments, and steering current equal to either 45% or 90% of the transverse excitation threshold generated a significant increase in the dynamic range and a significant increase in the maximum torque before spillover (Table II).

TABLE II
PARAMETERIZATION OF RECRUITMENT CHARACTERISTICS

PARAMETER	NO STEERING	NO *vs.* 45% MEAN DIFFERENCE *p*	45% STEERING	45% *vs.* 90% MEAN DIFFERENCE *p*	90% STEERING
Tripolar Current Threshold (μA)	1117±530 300-2600 (35,9)		635±348 200-1900 (23,6)		331±485 50-2600 (35,9)
Total Cathodic Current Threshold (μA)	1117±530 300-2600 (35,9)	231 *0.0001*	1351-535 415-2900 (23,6)	353 *0.0001*	1747±846 530-4600 (35,9)
NO *vs.* 90% MEAN DIFFERENCE *p*			646 *0.0001*		
Spillover Current (μA)	2286±995 800-4500 (35,9)	740 *0.0001*	3127±1284 915-6215 (23,6)	658 *0.0001*	3617±1603 1130-7430 (35,9)
NO *vs.* 90% MEAN DIFFERENCE *p*			1375 *0.0001*		
Dynamic Range (μA)	1169±758 300-3100 (35,9)	509 *0.0001*	1776±968 500-4050 (23,6)	305 *0.0001*	1869±1052 300-4300 (35,9)
NO *vs.* 90% MEAN DIFFERENCE *p*			729 *0.0001*		
Normalized Recruitment Gain	1.28±0.870 0-10.8 (23,6)	0.735 *0.0001*	0.513±0.375 0-4.966 (23,6)	0.285 *0.0002*	0.223±0.346 0.183-0.412 (23,6)
NO *vs.* 90% MEAN DIFFERENCE *p*			1.005 *0.0001*		
Maximum Absolute Torque (N-cm)	112±75 32-329 (35, 9)	11 *0.0406*	123±74 34-316 (23,6)	5 *0.0274*	128±77 35-323 (35,9)
NO *vs.* 90% MEAN DIFFERENCE *p*			16 *0.0149*		

Each entry in the table is the mean ± standard deviation of the parameter, the range of the parameter (min-max), and the number of samples (number of recruitment curves, number of experiments). Numbers between columns are the mean differences and p values for comparisons between no steering, 45% transverse steering, and 90% transverse steering using a two tailed, paired t-test.

5) Effects of Adjacent Steering Current: In three experiments the use of steering current from an electrode contact adjacent to the active cathode was investigated. For each of the four tripoles, recruitment curves were collected with no steering current, with 90% steering current from the transverse electrode contact [Fig. 1(c)], and with 90% steering current from either of the two adjacent electrode contacts [Fig. 1(d)]. Steering current from an adjacent anode altered the torques generated at the ankle joint indicating that it changed the pattern of excitation within the nerve trunk. Fig. 5 shows an example of the effects of adjacent steering current in one experiment. Tripole 270° was positioned at an intermediate location, closest to the CP fascicle but adjacent to the LG/S0 and MG fascicles. Without steering current, dorsiflexion torque was generated first, indicating activation of the CP fascicle, but spillover to the plantarflexors occurred before the torque reached a plateau. With 90% transverse steering (from the 90° contact) the maximum dorsiflexion torque and dynamic range were increased, but spillover occurred immediately after the maximum dorsiflexion torque was reached. With steering current from the adjacent electrode closest to the CP fascicle (from the 0° contact) spillover occurred at a lower current amplitude and lower torque value than without any steering current. Finally, with 90% steering current from the adjacent contact close to the plantarflexion innervation (from the 180° contact) the maximum dorsiflexion torque was generated, and spillover was prevented over the full range of stimulus currents that were tested. This example illustrates how adjacent steering current can be used to modify the region of excitation and thus control the torque that is generated by a particular tripole.

Analysis of 23 recruitment curves from three experiments indicated that adjacent steering current generated a significant increase in the dynamic range between threshold and spillover (mean increase = 720 μA, $p = 0.003$). In contrast to transverse steering current, adjacent steering current caused a decrease in the magnitude of the maximum dorsiflexion or plantarflexion torque generated before spillover (mean decrease = 11.5 N-cm, $p = 0.0372$, $n = 20$ pairs of recruitment curves where the first recruited fascicle did not change with use of 90% adjacent steering). Thus, in some

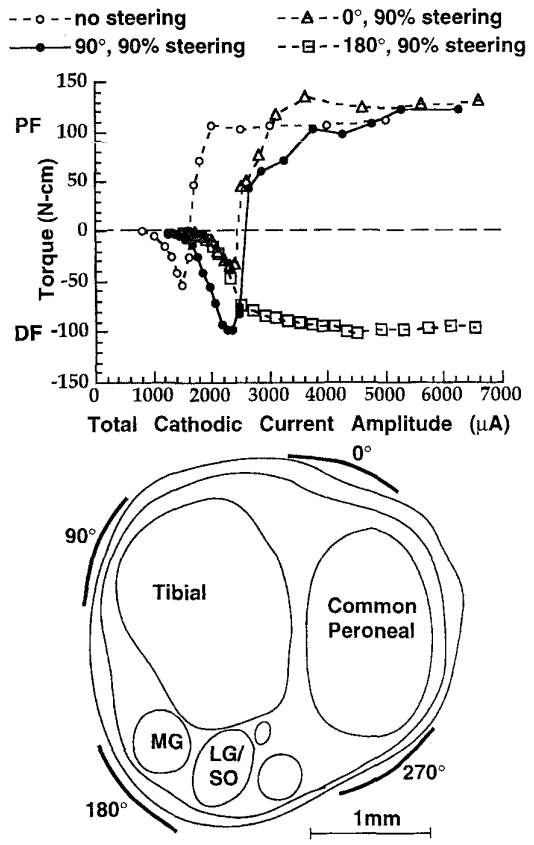

Fig. 5. Steering current from adjacent electrode contacts [Fig. 1(d)] changed the torque recruitment properties of the tripolar stimulus current. Recruitment curves of the plantarflexion/dorsiflexion (PF/DF) torque generated by activation with tripole 270° are plotted as a function of the total cathodic current (stimulating + steering) for four different conditions: no steering, 90% transverse steering current (1260 μA from contact at 90°), or 90% steering current from either of the two adjacent contacts (1620 μA from contact at 0° or 1512 μA from contact at 180°). Adjacent steering from the contact at 180° eliminated spillover over the range of amplitudes tested.

cases adjacent steering appeared to prevent full activation of the first recruited fascicle.

B. Functional Selectivity

1) Control of Joint Torque: The fascicle selectivity described above allowed selective and independent control of dorsiflexion and plantarflexion torques at the ankle joint using different tripoles within the cuff electrode in all nine experiments. Fig. 6 shows the combined results as a joint torque vector histogram in the PF/DF versus ER/IR plane calculated with a bin width of 5°. The border of the shaded region is the mean of the maximum torques achieved in each direction in each of the nine experiments, and the border of the open region indicates the addition of 1 standard deviation to the mean in each direction. The separability between PF/DF and ER/IR torques was dependent upon two factors: the direction of the torque vectors generated by individual muscles and the ability of the electrode to activate selectively each muscle. The limited separation between the two dimensions reflects the biomechanical actions of the active muscle(s) [22] not a lack of selectivity among the ankle musculature. Note

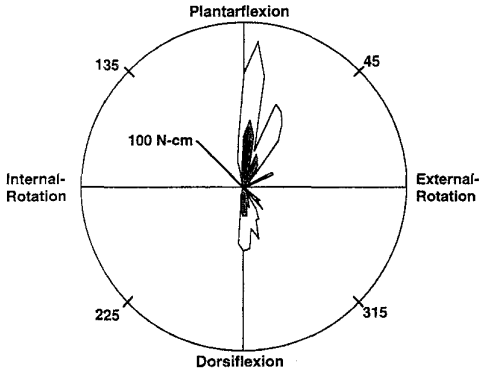

Fig. 6. Selective and independent control of dorsiflexion and plantarflexion torque was achieved in all nine experiments. The combined results of nine experiments are plotted as a histogram of joint torque vectors calculated with a bin width of 5°. The border of the shaded region indicates the mean of the maximum torques achieved in that direction in each of the nine experiments, and the border of the open region is the mean plus one standard deviation.

that the histogram exhibits three distinct modes: one between 60° and 70° indicative of MG activation, one between 80° and 90° indicative of LG/SO activation, and one between 265° and 275° indicative of activation of the dorsiflexor muscles innervated by the CP nerve [22]. Furthermore, the vectors in the second quadrant (plantarflexion/internal rotation) indicate activation of the plantaris (PL) which is innervated by the tibial nerve [1], [17].

The torques generated at the ankle depended on the static position of the joint. Ankle joint angle was defined between an imaginary line connecting the rotation centers of the knee and ankle and the dorsal surface of the paw [Fig. 1(b)]. Fig. 7 shows the magnitude and direction of the torques generated by two opposite tripoles at three different positions of the ankle joint [nerve topography shown in Fig. 3(h)]. Use of two tripoles allowed independent control of the PF/DF torque at the ankle joint [Fig. 7(b)]: tripole 0° generated plantarflexion torques and tripole 180° generated dorsiflexion torques. When the angle between the dorsal surface of the foot and the shank was changed, the magnitude of the torques generated by each tripole changed in opposite directions as expected from the length tension properties of skeletal muscle [28]. Angle dependent muscle moment arms also contributed to changes in torque output at different joint positions [44]. Finally, angle dependent changes in the recruitment properties of the electrode caused changes in the torque output. These changes arose from an alteration in the spatial relationship between the excitatory field generated by the electrodes and the excitable fibers, as would occur as a result of electrode movement. This last component is a characteristic of the electrode, not the physiological system, and was thus of particular interest in quantifying electrode performance.

C. Characteristics of Joint Torque Recruitment

1) Positional Stability: The effects of static changes in the ankle joint angle in the sagittal plane (plantarflexion/dorsiflexion direction) on recruitment were determined by measuring recruitment curves of joint torque as a function of stimulus amplitude at three ankle joint angles (70°, 90°, and 110°). The distribution of the position-dependent deviations

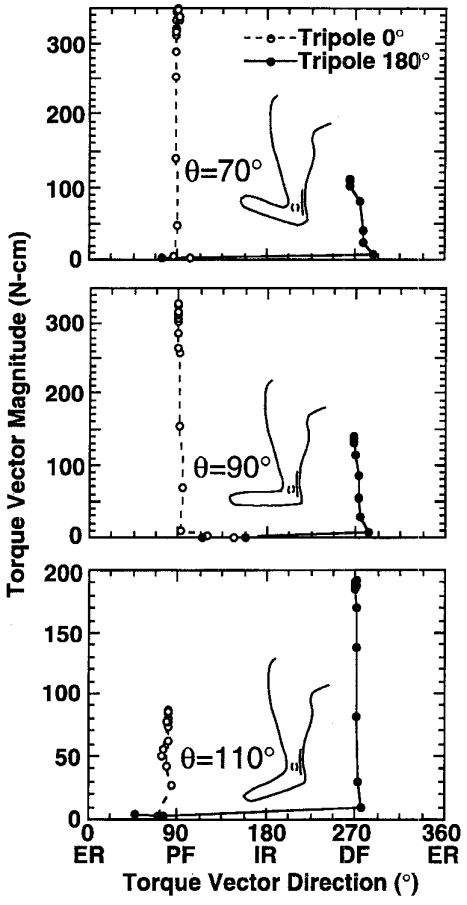

Fig. 7. The magnitude of the evoked torque depended on the ankle joint angle. Each panel shows the torque vector magnitude as a function of the torque vector direction generated by two different tripoles at three initial positions of the ankle joint (ER = external rotation, IR = internal rotation, PF = plantarflexion, DF = dorsiflexion). (a) 70°. (b) 90°. (c) 110°.

(see METHODS) from 28 pairs of recruitment curves collected in five different experiments is shown in Fig. 8 (mean absolute deviation = $8.8 \pm 9.8\%$, $n = 209$ points). Neither the absolute nor the relative deviation was correlated with either the relative torque magnitude ($r^2 = 0.011$) or the absolute torque magnitude ($r^2 = 0.021$). Additionally, the deviations were not significantly different between cases where the active muscle was either lengthened ($n = 108$) or shortened ($n = 101$), ($p = 0.9543$ for absolute deviation, $p = 0.5606$ for relative deviation, unpaired 2-tailed t-test), or between different directions of joint angle change ($p = 0.1315$ for absolute deviation, $p = 0.4184$ for relative deviation, unpaired 2-tailed t-test). The mean deviation between repeated measurements at the same joint angle, before and after a static change in joint angle, ($13.2\% \pm 15.5$, $n = 55$ points over eight recruitment curves in three animals) was larger ($p = 0.0052$, 1 tailed unpaired t-test) than the mean error between measurements at the two different joint angles ($8.8 \pm 9.8\%$, $n = 209$). These results suggest that the deviations resulted from small shifts in electrode position that occurred when the joint angle was changed, and indicate that the deviation was not a systematic error resulting from consistent changes of fiber to electrode distance that occurred as the joint was moved.

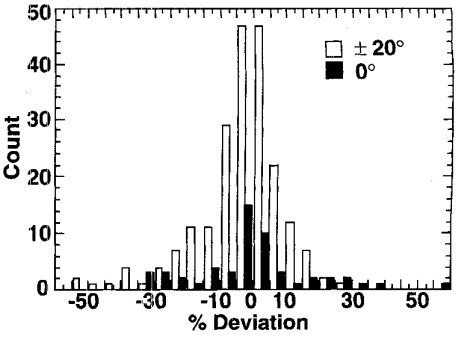

Fig. 8. Recruitment was measured at three different ankle joint angles to quantify position dependent recruitment properties. Histogram of the distribution of the deviations between recruitment measured at 90° and recruitment measured at 70° or 110° (28 pairs of recruitment curves from five experiments), and errors between repeated measurements at 90° after an intervening change in ankle joint angle (eight pairs of recruitment curves from three experiments).

2) Recruitment Gain: The electrode allowed graded control of joint torque by modulating the amplitude of the tripolar stimulus current (Figs. 3 and 7). The ability to grade contractions was quantified by calculating the normalized recruitment gain (i.e., slope) over each recruitment curve (Table II). Transverse field steering current significantly reduced the mean value and range of the normalized recruitment gain (NRG) over a recruitment curve. When compared as a group, recruitment curves with steering current at either 45% or 90% had significantly lower mean values of NRG and significantly smaller ranges of NRG than recruitment curves collected without steering current (Table II).

IV. Discussion

A multiple contact nerve cuff electrode implanted on the sciatic nerve was used to control the torque generated at the ankle joint by selective activation of individual nerve fascicles. Anatomical variability precluded placing the cuffs in the same relative location in every experiment, and no effort was made to align the electrode contacts over specific nerve regions. To overcome anatomical variability, McNeal and Bowman [25] tuned the position of a sleeve electrode with respect to the desired response during the implant procedure. We decided against this approach because such tuning would depend strongly on the nerve structure, and would therefore make pooling of data for statistical comparisons difficult. More practically, transduction of the stimulated functions is required for tuning of the electrode orientation. In a clinical application, it will be difficult to provide per-operative transduction of the stimulated response, and there may be changes in the stimulated response over time as a result of tissue encapsulation [13], [15] and systemic physiological adaptations (e.g., muscle conditioning, changes in joint stiffness). We therefore implanted electrodes without prior reference to fascicular location to eliminate problems with pooling data and to model as closely as possible the anticipated clinical situation.

Low frequency trains of short duration rectangular pulses were used to evoke twitch contractions in the ankle musculature. Short pulsewidths were selected to increase the threshold difference between different diameter nerve fibers,

thereby reducing recruitment gain [9], and to increase the threshold difference between fibers at different distances from the electrode, thereby increasing spatial selectivity [16]. We chose to use single pulse stimulation to minimize the effects of fatigue during the long time course of the experiments.

No effort was made to tune stimulus parameters or electrode configurations to achieve selective activation of a specific fascicle. Retrospective analysis of joint torque data and neural topography suggested that tuning procedures would have further improved selectivity. However, such tuning would create a unique data set for each experiment and preclude pooling of results for statistical analysis. Because a consistent set of electrode configurations and stimulus parameters were tested in each experiment, our data set included a large number of recruitment curves from nine experiments. The quantitative parameters that we used to describe each curve (dynamic range, maximum torque, plateau width, and recruitment gain) allowed us to compare statistically, with significant results, the performance of the cuff under different conditions (e.g., with and without steering).

These analyses indicated that steering current increased the spatial selectivity of activation with the cuff electrode. Transverse steering current restricted activation to a smaller region of the nerve trunk by increasing the current amplitude at which spillover occurred. This was demonstrated by the increased dynamic range between threshold and spillover (Table II) and the increased slope of the current distance relationship with steering current (Fig. 4). Steering current also allowed activation of more fibers within a localized region of the nerve trunk as shown by the increases in maximum force before spillover (Table II). The increases in these quantitative performance measures resulted in a larger region of stimulating currents over which the torque was a monotonically increasing function of the stimulus current amplitude. However, they come at the cost of an increase in total cathodic current (Table II). The increased current requirements make more charge available to drive irreversible electrochemical reactions, and this additional charge must be recovered during the second phase of the stimulus to avoid electrode corrosion and tissue damage [29].

There are two mechanisms by which steering current increased selectivity. Modeling studies have demonstrated that transverse steering current increases the current density under the active cathode [4], [33]. This mechanism was evident by decreases in the tripolar current thresholds (Table II), increases in the slope of the current distance curve (Fig. 4), and increases in the maximum torque using transverse steering current (Table II). The results with adjacent steering electrodes demonstrated the second effect of steering current which was to hyperpolarize the nerve fibers near the steering anode. This anodal hyperpolarization reduced the depolarizing effect of the coincident stimulus pulse, thus elevating threshold for fibers near the steering anode. This was reflected by the increased dynamic range when using transverse steering current (Table II), by the changes in patterns of spillover with adjacent steering current (Fig. 5), and in some cases by a reduction in the maximum torque that could be generated when using adjacent steering current. This effect is analogous to the sharpening of excitation fields by anodal currents in cochlear prostheses [36].

Stimulation of discrete regions of the nerve trunk with different tripoles allowed selective and graded control of dorsiflexion and plantarflexion torques in all nine experiments. Comparisons between stimulation with the cuff electrode and stimulation of individual branches with a hook electrode demonstrated that the cuff can stimulate entirely a single branch of the nerve before spillover occurred. Several other types of electrodes have been developed for stimulation of peripheral nerve [27]. However, comparable experimental studies of selective activation of multiple muscles are scarce. Electrodes sutured to the epineurium have been used to activate the phrenic nerve in a diaphragm pacing application [35] and the femoral nerve for ambulation [20], but few data have been published to demonstrate the degree of selectivity available with this approach [19]. Modeling studies have suggested that intrafascicular electrodes allow more selective activation of nerve trunk regions than extraneural electrodes [40], but this prediction has yet to be demonstrated experimentally. The results of Veltink *et al.* [39] indicated that the tibialis anterior and extensor digitorum longus muscles of rat were recruited simultaneously by electrodes placed within the peroneal nerve, and the data of Koole *et al.* [21] demonstrated a limited degree of selectivity between the tibial and common peroneal fascicles of the rat sciatic nerve with intrafascicular wire electrodes. Yoshida and Horch [43] reported limited overlap between activation of two fascicles (0.8–15.6% of maximum force) using individual intrafascicular wire electrodes, but the maximum forces (12.9 ± 2.9 N) suggest that two electrodes, even when maximally activated, were not stimulating the entire fascicle.

The multiple contact nerve cuff electrode allowed graded control of joint torque. The recruitment gains measured in this study (0.22 with steering to 1.28 without steering) are within the ranges estimated from data reported for intrafascicular stimulation (0.21–1.2) and extraneural stimulation (1.85–2.4) using 60 μs rectangular pulses [39]. Also, the values measured in the present study are in the lower part of the range of recruitment gains reported for epimysial electrodes using 100 μs rectangular pulses (0.2–4.5) [11]. The lower values of recruitment gain found in the present study resulted from the very short pulsewidths that were used (10 μs). Previous studies have indicated that short pulsewidths increase the threshold difference between fibers of different diameter, and thus allow recruitment to be graded more easily [9]. Additionally, short pulsewidths increase the threshold difference between fibers of the same diameter lying at different distances from the electrode (i.e., increase the slope of the current distance relationship) [16], and this may contribute to the ability to grade activation levels. Steering current also reduced the magnitude and range of the recruitment gain. This resulted from the increase in the slope of the current-distance curve with steering current, which increased the threshold difference between different nerve fibers within the active muscle's region of innervation.

The patterns of fascicle selectivity, and thus joint torque recruitment, were dependent on the distance between the electrode contacts and the nerve fibers (Fig. 4). However, our results suggest that approximately 50% of the variation in threshold current was due to factors other than the electrode to

fiber distance. Previous modeling studies have indicated that the inhomogeneous and anisotropic electrical conductivity of the nerve tissues affect the recruitment patterns during extraneural stimulation [2], [4], [38], [40]. Similarly, theoretical and experimental studies have demonstrated that variations in neural geometry will affect the recruitment order of the fascicles (Fig. 3) [33], [39], [40], [41]. The nonuniform current density on the electrode contacts may also have affected the current-distance relationship. However, we obtained similar results whether the distance to the fascicle was measured from the center of the contact (where the current density is lowest) or the edge of the contact (where the current density is highest) ($r^2 = 0.42$ without steering and $r^2 = 0.46$ with steering for linear fit), which suggests that this was not a major factor. The variation in diameter of the first recruited nerve fibers could also affect the current distance relationship (i.e., the first recruited fibers may not lie at the closest edge of the fascicle). To test this possibility we restricted our analysis to the MG and LG/SO fascicles which are much smaller than the CP and TIB fascicles. The results of this restricted analysis (42 points, $r^2 = 0.54$ without steering and $r^2 = 0.53$ with steering, for linear fit) indicated that this was most likely a minor factor in the empirical current-distance relationship. Thus, the most likely sources of threshold variability, along with the electrode to fiber distance, are the geometry and electrical properties of the nerve trunk.

The measurements of recruitment properties at different ankle joint positions indicated that there was some degree of position dependent recruitment. Although 80% of the deviations were less than 20% of the maximum torque, this amount of position dependence was not expected. One compounding factor in the analysis is the assumption that the length-tension properties of all active motor units are the same. Experimental results in cat peroneus longus indicate that at least 70% of motor units have optimal lengths within 1.5 mm of the whole muscle optimal length [7]. Further, the optimal lengths of the large, high force producing motor units were closest to the optimal length of the whole muscle [7], [23]. Therefore, this assumption will only introduce small, nonsystematic changes in torque output and does not affect the conclusion that there is relative movement between the electrodes and the nerve fibers during changes in limb position. A previous report indicated that changes in muscle length, rather than limb position, did not cause changes in nerve cuff recruitment properties [6]. The changes in joint angle used here, however, are more like limb movements that would occur during application of a cuff electrode in motor prostheses systems. More recent experiments with chronically implanted cuff electrodes indicate that tissue encapsulation stabilizes the electrode position and reduces significantly the degree of position dependent recruitment [14].

The present results demonstrate that a multiple contact extraneural cuff allowed selective and independent activation of multiple fascicles within a large nerve trunk when placed without prior reference to fascicle location and without tuning of the stimulus parameters or electrode geometry. The addition of more electrode contacts to the cuff would be expected to improve selectivity. This assertion is supported by previous results showing that a virtual tripole at an intermediate location allowed selectivity that was other not otherwise attainable [41]. Also, the results of the present study indicating that selectivity was dependent on nerve geometry, and that the threshold difference between neighboring fascicles was dependent on the electrode to fiber distance, suggest that additional contacts would improve selectivity. This improvement, however, would come at the cost of additional lead wires from the cuff. The choice of the number of contacts to be implemented is strongly dependent on the particular application, and if additional contacts are to be added to similarly sized electrodes, it will require modifications to the current fabrication technology.

The level of selectivity and the input-output characteristics of the electrode make it suitable for application in a motor prosthesis. Implementation of a twelve-contact electrode, as used here, would require two isolated stimulator output stages (one for stimulating current and one for steering current) and a switching network to connect the stimulators to the appropriate electrode contacts. Before application in a clinical motor prosthesis, future work must address the temporal and positional stability of recruitment properties of a chronically implanted nerve cuff electrode [14], [15], and document the tissue response to the long-term presence of the electrode.

ACKNOWLEDGMENT

The authors would like to thank Drs. D. Durand, P. H. Peckham, and C. Veraart for comments on earlier versions of this manuscript; H. Kayyali for fabrication and maintenance of the stimulator used in these studies; M. Miller for development of data collection software; J. Polak and K. Petonovich for histological processing, and D. Tyler for assistance during experiments.

REFERENCES

[1] D. D. Abraham and G. E. Loeb, "The distal hindlimb musculature of the cat: Patterns of normal use," *Exp. Brain Res.*, vol. 58, pp. 580–593, 1985.

[2] K. W. Altman and R. Plonsey, "Point source nerve bundle stimulation: Effects of fiber diameter and depth on simulated excitation," *IEEE Trans. Biomed. Eng.*, vol. 37, pp. 688–698, 1990.

[3] G. S. Brindley, C. E. Polkey, and D. N. Rushton, "Sacral anterior root stimulators for bladder control in paraplegia," *Paraplegia*, vol. 20, pp. 365–381, 1982.

[4] R. R. Chintalacharuvu, D. A. Ksienski, and J. T. Mortimer, "A numerical analysis of the electric field generated by a nerve cuff electrode," in *Proc. 13th Int. Conf. IEEE-EMBS*, vol. 13, 1993, pp. 912–913.

[5] P. E. Crago and P. H. Peckham, and G. B. Thrope, "Modulation of muscle force by recruitment during intramuscular stimulation," *IEEE Trans. Biomed. Eng.*, vol. 27, pp. 679–684, 1980.

[6] W. K. Durfee and K. I. Palmer, "Estimation of force-activation, force-length, and force-velocity properties in isolated electrically stimulated muscle," *IEEE Trans. Biomed. Eng.*, vol. 41, pp. 205–216, 1994.

[7] G. M. Filippi and D. Troiani, "Relations among motor unit types, generated forces and muscle length in single motor units of anesthetized cat peroneus longus muscle," *Exp Brain Res.*, vol. 101, pp. 406–414, 1994.

[8] W. W. L. Glenn and M. L. Phelps, "Diaphragm pacing by electrical stimulation of the phrenic nerve," *Neurosurgery*, vol. 17, pp. 974–984, 1985

[9] P. H. Gorman and J. T. Mortimer, "The effect of stimulus parameters on the recruitment characteristics of direct nerve stimulation," *IEEE Trans. Biomed. Eng*, vol. 30, pp. 407–414, 1983.

[10] G. E. Goslow Jr., R. M. Reinking, and D. G. Stuart, "The cat step cycle: Hindlimb joint angles and muscle lengths during unrestrained locomotion," *J. Morphology*, vol. 141, pp. 1–42, 1973.

[11] P. A. Grandjean and J. T. Mortimer, "Recruitment properties of monopolar and bipolar epimysial electrodes," *Ann. Biomed. Eng.*, vol. 14, pp. 53–66, 1986.
[12] W. M. Grill and J. T. Mortimer, "Functional control of joint torque with a cuff electrode," in *Proc. 15th Int. Conf.*, IEEE-EMBS vol. 15, 1993, pp. 1328–1329.
[13] ——, "Electrical properties of implant encapsulation tissue," *Ann. Biomed. Eng.*, vol. 22, pp. 23–33, 1994.
[14] ——, "Postional dependence of the recruitment properties of nerve cuff stimulating electrodes," in *Proc. 1995 Conf. Rehab. Eng. Soc. North Am.*, 1995, pp. 717–719.
[15] ——, "Temporal stability of nerve cuff electrode recruitment properties," in *Proc. 17th Int. Conf.*, IEEE-EMBS no. 403, 1995.
[16] ——, "The effect of stimulus pulse duration on selectivity of neural stimulation," *IEEE Transactions on Biomedical Engineering*, vol. 43, pp. 161–166, 1996.
[17] ——, "Non-invasive measurement of the input output properties of peripheral nerve stimulating electrodes," *J. Neuroscience Methods*, vol. 65, pp. 43–50.
[18] F. T. Hambrecht, "Neural prostheses," *Ann. Rev. Biophys. Bioeng.*, vol. 8, pp. 239–267, 1979.
[19] W. Happak, H. Gruber, J. Holle, W. Mayr, Ch. Schmutterer, U. Windborg, and H. Thoma, "Multi-channel indirect stimulation reduces muscle fatigue," in *Proc. 11th Int. Conf.*, IEEE-EMBS vol. 11, 1989, pp. 240–241.
[20] J. Holle, H. Thoma, M. Frey, H. Gruber, H. Kern, and C. Schwanda, "Walking with an implantable stimulation system for paraplegics," in *Proc. 2nd Int. Conf. on Rehab. Eng.*, Ottawa, Canada, 1984.
[21] P. Koole, J. H. M. Put, P. H. Veltink, and J. Holsheimer, "Muscle selective nerve stimulation for FES," in *Proc. 1989 Vienna Workshop FES*, 1989, pp. 155–158.
[22] J. H. Lawrence III, T. R. Nichols, and A. W. English, "Cat hindlimb muscles exert substantial torques outside the sagittal plane," *J. Neurophys.* vol. 69, pp. 282–285, 1993.
[23] D. M. Lewis and J. C. Luck, "Effect of initial length on the tension developed by motor units in flexor hallicus longus muscle of cat," *J. Physiol.*, vol. 197, 42P-43P, 1968.
[24] G. E. Loeb, "Neural prosthetic interfaces with the nervous system," *Trends Neurosci.*, vol. 12, pp. 195–201, 1989.
[25] D. R. McNeal and B. R. Bowman, "Selective activation of muscles using peripheral nerve electrodes," *Med. and Biol. Eng. and Comp.*, vol. 23, pp. 249–253, 1985.
[26] I. Miller, J. E. Freund, and R. A. Johnson, *Probability and Statistics for Engineers*, IVth ed., Englewood Cliffs, NJ: Prentice-Hall, pp. 240–248, 304–306, 1990.
[27] J. T. Mortimer, W. F. Agnew, K. Horch, P. Citron, G. Creasey, and C. Kantor, "Perspectives on new electrode technology for stimulating peripheral nerves with implantable motor prostheses," *IEEE Trans. Rehab. Eng.* vol. 3, pp. 145–154, 1995.
[28] P. M. H. Rack and D. R. Westbury, "The effects of length and stimulus rate on tension in the isometric cat soleus muscle," *J. Physiol.*, vol. 204, pp. 443–460, 1969.
[29] L. S. Robblee and T. L. Rose, "Electrochemical guidelines for selection of protocols and electrode materials for neural stimulation," in *Neural Prostheses: Fundamental Studies*, W. F. Agnew and D. B. McCreery, Eds., Englewood Cliffs, NJ: Prentice-Hall, 1990.
[30] W. L. C. Rutten, H. J. van Wier, and J. H. M. Put, "Sensitivity and selectivity of intraneural stimulation using a silicon electrode array," *IEEE Trans. Biomed. Eng.*, vol. 38, pp. 192–198, 1991.
[31] R. A. Schmidt, H. Bruschini, and E. A. Tanagho, "Micturition and the male genitourinary response to sacral root stimulation," *Invest. Urol.*, vol. 17, pp. 125–129, 1979.
[32] R. B. Stein, P. H. Peckham, and D. B. Popovic, *Neural Prostheses: Replacing Motor Function After Disease or Disability*. NY: Oxford University Press, 1992.
[33] J. D. Sweeney, D. A. Ksienski, and J. T. Mortimer, "A nerve cuff technique for selective excitation of peripheral nerve trunk regions," *IEEE Trans. Biomed. Eng.*, vol. 37, pp. 706–715, 1990.
[34] P. P. Talonen, G. A. Baer, V. Häkkinen, and J. K. Ojala, "Neurophysiological and technical considerations for the design of an implantable phrenic nerve stimulator," *Med. Biol. Eng. Comput.*, vol. 28, pp. 31–37, 1990.
[35] H. Thoma, W. Girsch, J. Holle, and W. Mayr, "The phrenic pacemaker: Substitution of paralyzed functions in tetraplegia," *Trans. Am. Soc. Artif. Internal Organs.*, vol. 10, pp. 472–479, 1987.
[36] B. Townshend and R. L. White, "Reduction of electrical interaction in auditory prostheses," *IEEE Trans. Biomed. Eng.*, vol. 34, pp. 891–897, 1987.
[37] D. J. Tyler and D. M. Durand, "Design and acute test of a radially penetrating interfascicular nerve electrode," in *Proc. 15th Int. Conf.*, IEEE-EMBS vol. 15, 1993, pp. 1247–1248.
[38] P. H. Veltink, J. A. van Alste, and H. B. K. Boom, "Influences of stimulation conditions on recruitment of myelinated nerve fibers: A model study," *IEEE Trans. Biomed. Eng.*, vol. 35, pp. 917–924, 1988.
[39] ——, "Multielectrode intrafascicular and extraneural stimulation," *Med. Biol. Eng. Comput.*, vol. 27, pp. 19–24, 1989.
[40] P. H. Veltink, B. K. Van Veen, J. J. Struijk, J. Holsheimer, and H. B. K. Boom, "A modeling study of nerve fascicle stimulation," *IEEE Trans. Biomed. Eng.*, vol. 36, pp. 683–691, 1989.
[41] C. Veraart, W. M. Grill, and J. T. Mortimer, "Selective control of muscle activation with a multipolar nerve cuff electrode," *IEEE Trans. Biomed. Eng.*, vol. 40, pp. 640–653, 1993.
[42] R. L. Waters, D. R. McNeal, W. Faloon, and B. Clifford, "Functional electrical stimulation of the peroneal nerve for hemiplegia," *J. Bone Joint Surg.*, vol. 67-A, p. 792, 1985.
[43] K. Yoshida and K. Horch, "Selective stimulation of peripheral nerve fibers using dual intrafascicular electrodes," *IEEE Trans. Biomed. Eng.*, vol. 40, pp. 492–494, 1993.
[44] R. P. Young, S. H. Scott, and G. E. Loeb, "An intrinsic mechanism to stabilize posture: Joint-angle-dependent moment arms of the feline ankle muscles," *Neur. Lett.*, vol. 145, pp. 137–140, 1992.

Warren M. Grill Jr. (M'95) was born in Plainfield, NJ in 1967. He received the B.S. degree in biomedical engineering with honors in 1989 from Boston University, Boston, MA. He earned the M.S. degree and the Ph.D. degree, both in biomedical engineering, from Case Western Reserve University, Cleveland, OH in 1992 and 1995, respectively. He has received student paper awards from both the IEEE EMBS and RESNA. During the summer of 1995 he attended a course on Neural Systems and Behavior at the Marine Biological Laboratory, Woods Hole, MA.

He is presently a Research Associate in the Department of Biomedical Engineering at Case Western Reserve University. His research interests include neural prostheses, the electrical properties of tissues and cells, computational neuroscience, and neural control.

Dr. Grill is a member of the IEEE, the Biomedical Engineering Society, and the Society for Neuroscience.

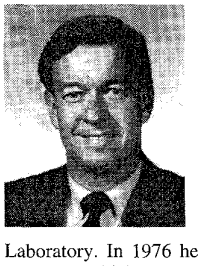

J. Thomas Mortimer, a native of Texas, received the B.S.E.E. degree from Texas Technological College, the M.S. degree from Case Institute of Technology, and the Ph.D. degree from Case Western Reserve University in Cleveland, OH.

He was Visiting Research Associate at Chalmers Tekniska Hogskola, Göteborg, Sweden, from 1968 to 1969. He then joined the Department of Biomedical Engineering at Case Western Reserve University, where he currently holds the title of Professor. He is also the Director of the Applied Neural Control Laboratory. In 1976 he was awarded the Humboldt-Preis by the Alexander von Humboldt Foundation, Federal Republic of Germany. In 1977–78 he was a Visiting Professor at the Institute für Biokybernetik und Biomedizinische Technik, Universität Karlsruhe, Karlsruhe, West Germany. In 1992 he was a Visiting Scholar at Tohoko University, Sendai, Japan. He is a Founding Fellow of the American Institute for Medical and Biological Engineering. His research interests concern electrically activating the nervous system. He holds nine patents in this area and has over 70 publications dealing with neural prostheses and related to pain suppression, motor prostheses for restoration of limb function and respiration, bladder and bowel assist, electrode, tissue damage and methods of selective activation. He is President of Axon Engineering, Inc. in Willoughby, Ohio, a company providing electrodes and consulting services to parties interested in developing new products in the neural prosthesis area.